

## ATR-FTIR spectroscopy as a probe for metal ion binding onto immobilized ligands

Spiro D. Alexandratos<sup>1,2\*</sup> and Xiaoping Zhu<sup>1</sup>

<sup>1</sup>*Dept. of Chemistry, Hunter College of the City University of New York, 695 Park Ave., New York, NY 10065;* <sup>2</sup>*The Ph.D. Program in Chemistry, Graduate Center of the City University of New York, New York, NY 10016*

### ABSTRACT

ATR-FTIR spectroscopy is shown to be useful in probing metal ion binding to ligands immobilized on polymer beads. Lu(III) is the metal ion, phosphinic and sulfonic acids are the immobilized ligands, and polystyrene beads crosslinked at low and high levels are the support. Analysis is based on ligand band positions and intensities before and after complexation as a function of time. ATR spectra of the phosphinic acid show two types of binding sites with different accessibilities: surface ligands that bind Lu(III) from solution and interior ligands that gain ions by diffusion from the surface. Initially bound Lu(III) ions are mobile within the solid phase and their movement is accompanied by the breaking of hydrogen bonds among the phosphinic acid ligands to form Lu(III) phosphinate complexes. Competition between hydrogen bonding and bond-making with Lu(III) contributes to slow sorption rates compared to results from the sulfonic acid ligand whose strong acidity and ionizability allows rapid Lu(III) sorption. Comparing ATR spectra of the phosphinic acid bound to lightly- and highly-crosslinked polystyrene shows how the extent of crosslinking affects the transport mechanism.

*Keywords:* polymer; functional material; separations; ion exchange; FTIR

---

\* Corresponding author: alexsd@hunter.cuny.edu

## 1. Introduction

Environmental remediation of surface and ground water is a major problem.<sup>1</sup> Pretreatment of waste solutions for the recovery of metals before their discharge into the environment has resulted in the development of metal recovery methods.<sup>2</sup> Among widely used technologies, sorption with chelating resins is important to recovering metal ions from multi-component solutions.<sup>3</sup> Selectivity is due to the complexing properties of functional groups bound to the polymer<sup>4</sup> and there is significant effort in preparing new ion-selective sorbents<sup>5</sup> as well as in understanding metal-ligand interaction mechanisms.<sup>6</sup> While sorbents with unique metal affinities and high sorption capacities are promising for efficient metal ion separations from aqueous solutions, knowing the mechanisms of interaction is important in order to combine high metal ion affinities with rapid sorption kinetics.<sup>7</sup> A study of metal ion sorption can thus provide a better understanding of the interaction between metal ions in solution and sites on the solid as well as methods to maximize loading.

Metal ion adsorption is usually observed to be rapid at the start of contact and then slower as equilibrium is approached. Given a sorbent with internal and external adsorption sites, mass-transfer and adsorption-reaction models describe this process as following four steps: (i) transport of the ion from bulk solution to the surface of the adsorbent; (ii) interphase (film) mass transfer; (iii) diffusion inside the solid (intra-particle diffusion); and (iv) reaction on the adsorption sites.<sup>8</sup> Any of these steps can be rate-limiting and control the overall adsorption rate.<sup>9,10,11</sup> This rate depends on the difference between the amount of adsorbed metal ion at a given time and the equilibrium capacity. Kinetic models may follow pseudo-first or -second order equations.<sup>12</sup>

Adsorption of metal ions onto functionalized polymers is affected by factors that include ligand density,<sup>13</sup> accessibility,<sup>14</sup> support properties,<sup>15</sup> ionic strength,<sup>16</sup> and other solution conditions<sup>17</sup> and is accompanied by the formation of new ionic and/or coordinate covalent bonds.<sup>18</sup> An understanding of the metal-ligand interaction is necessary to model its adsorption mechanism and this has been studied with a range of techniques, including EDX,<sup>19</sup> reflectance,<sup>20</sup> luminescence,<sup>21</sup> EPR,<sup>22</sup> UV-vis<sup>23</sup> and EXAFS.<sup>24</sup> In all cases, the equilibrium structure of the metal ion with the ligand is characterized. However, adsorption is complicated by the fact that sites

are not equally available for binding with some being on the surface but most being inside the solid. Particle diffusion and chemical reaction models usually do not account for inhomogeneity but are based on the change of metal ion concentration in solution which gives the total amount of metal transferred to the solid but not where binding occurs. Following metal ion transfer within the solid phase yields a better understanding of adsorption.

Metal ion uptake on functionalized polymers occurs with the formation of new bonds which suggests that FTIR spectroscopy can be a readily available means for monitoring adsorption through changes in the bands of metal-free and metal-loaded functional groups. Additionally, ATR-FTIR provides a unique opportunity for observing adsorption on polymers when done as a function of time. Since the penetration depth of the evanescent wave is  $< 1.5 \mu\text{m}$ , ATR-FTIR can probe solid /liquid interfacial phenomena.<sup>25,26</sup> Using polymer beads with diameters of 250-595  $\mu\text{m}$ , spectra will reflect adsorption only on their surface.

In this report, ATR-FTIR spectroscopy is used to characterize the adsorbent after contact with the metal ion at different times and different concentrations in order to visualize transport of the ion into the matrix. This continues our research with FTIR spectroscopy on crosslinked polymers that defines the utility of the mid-IR region within  $800 - 2800 \text{ cm}^{-1}$  where significant bands from the ligands appear.<sup>27</sup> Since soluble<sup>28</sup> and immobilized<sup>29</sup> phosphorus-based ligands have good metal ion selectivity, the simple phosphinic acid was chosen for this study bound to polystyrene beads as the adsorbent. As such, it serves as the model for more complex phosphorus-based ligands to be studied. FTIR has shown polystyrene-bound phosphorus acids to break their inter-ligand hydrogen bonds when binding metal ions through ion exchange and coordination.<sup>30</sup> This is seen through shifts in the P=O and P-O(H) bands as well as a new band between the two assigned to the POO(M)<sup>27</sup> thus displaying the applicability of ligand band changes as indicators of complexation in crosslinked polymers, especially with phosphorus-based ligands (lanthanide-phosphonate bands are not evident in the expected far-IR region due to strong ionic bonding).<sup>31</sup> Polystyrene-bound sulfonic acid was also studied to note the effect of acid strength on adsorption. Their structures are shown in Fig. 1. The polystyrene matrix for both was crosslinked with 2 wt% divinylbenzene. Finally, the effect of a tighter matrix was determined with XAD-4 functionalized with phosphinic acid.

The metal ion chosen for this study was Lu(III) which is a hard cation, as are all lanthanides, and so its coordinate structure is rather straightforward due to a weak stereochemical preference.<sup>32</sup> It has a high affinity for phosphorus-based ligands<sup>33</sup> and its binding to phosphinic acid is evident with a new band at 1057 cm<sup>-1</sup> assigned to POO(Lu).<sup>27</sup>

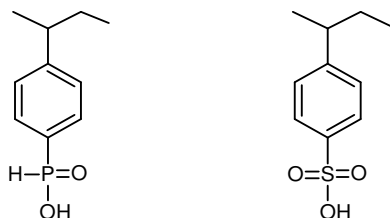


Fig. 1. Structures of polystyrene-bound phosphinic (left) and sulfonic (right) acids

## 2. Materials and Methods

**Materials.** Styrene, divinylbenzene (DVB), anhydrous AlCl<sub>3</sub>, PCl<sub>3</sub>, chlorosulfonic acid, solvents, Lu(NO<sub>3</sub>)<sub>3</sub> and lutetium atomic absorption standard solution were purchased from Sigma-Aldrich or Fisher Scientific and used directly without further treatment.

**Preparation of polystyrene beads.** The preparation of microporous (gel) polystyrene beads crosslinked with 2 wt% DVB by suspension polymerization has been described.<sup>34</sup> The beads were extracted with toluene in a Soxhlet extractor. After oven-drying, the beads were sieved to a particle size of 250-595 µm (i.e., 30-60 mesh).

**Preparation of gel phosphinic acid.** Polystyrene beads (10.0 g) were swelled in 100 mL of PCl<sub>3</sub> for 1 h in a 500 mL round-bottom flask fitted with a condenser, overhead stirrer and N<sub>2</sub> gas inlet tube. Aluminum chloride was added slowly over a period of 30 min and the mixture stirred at 23°C for 17 h. The flask was then placed in an ice bath and water added dropwise until all remaining PCl<sub>3</sub> and AlCl<sub>3</sub> was hydrolyzed. The HCl gas produced was directed into 6 M NaOH with a nitrogen gas flow. The beads were washed with 100 mL of 6 M HCl, then water until neutral, and conditioned in a glass frit funnel with 1 L of each 1 M NaOH, H<sub>2</sub>O, 1 M HCl and H<sub>2</sub>O.

**Preparation of gel sulfonic acid.** Polystyrene beads (5.0 g) were swelled in 100 mL of 1,2-dichloroethane for 1 h in a 250 mL round-bottom flask fitted with a condenser and overhead

stirrer; 10 mL of chlorosulfonic acid was added and the reaction refluxed for 17 h. The beads were washed with 100 mL each of dichloroethane, methanol, water and conditioned as above.

**Characterization.** The acid capacities of the phosphinic and sulfonic acid beads were determined by stirring 0.50 g of each dried on a Buchner funnel with 50 mL 0.1000 M NaOH containing 5% NaCl for 17 h and then titrating a 10 mL aliquot with 0.1000 M HCl. The percent solids (i.e., oven-dry bead weight divided by Buchner-dry weight  $\times$  100) was determined by Buchner-drying beads for 5 min to remove excess water (wet weight) and then oven-drying at 110 °C for 17 h (dry weight). The phosphorus capacity was determined by mineralizing 20 mg dry beads in concentrated H<sub>2</sub>SO<sub>4</sub> in the presence of CuSO<sub>4</sub> and subsequent reaction with ammonium vanadate-molybdate.<sup>35</sup> The intensity of yellow coloration was measured at 470 nm on a Spectronic 21D (Milton Roy) and the phosphorus determined from a calibration curve.

**Adsorption kinetics.** Enough beads to give 0.50 mmol P or the equivalent acid capacity were contacted with 50 mL of solution containing 0.033, 0.10, 0.50 or 1.0 mM Lu(III) in 0.01 M HNO<sub>3</sub>. At given times (see Results section), the solution was removed from the beads and the Lu(III) concentration determined by inductively coupled plasma atomic emission spectrometry (ICP-AES, Perkin-Elmer Optima 7000V). After complete removal of solution from the flask and washing the beads with water, the Lu(III)-loaded beads were further contacted with 20 mL of water for 17 h. Sequential loading was determined by contacting 50 mL of 0.50 mM Lu(III) with beads for 1 h, then removing the solution to measure its Lu(III) concentration, washing the beads with water and again contacting with 50 mL of 0.50 mM Lu(III). This was repeated 5 times. The percent sorption was calculated from the Lu(III) concentration before and after contact.

**ATR-FTIR.** Spectra were taken on a PerkinElmer Spectrum 65. The ATR accessory is equipped with a trapezoidal ZnSe crystal as the internal reflection element; 16 scans with a resolution of 4 cm<sup>-1</sup> were averaged for each spectrum.

### 3. Results

The phosphinic acid polymer has acid and phosphorus capacities of 5.20 and 4.96 mmol/g, respectively, indicating complete functionalization to the primary phosphinic acid; the sulfonic acid is also fully functionalized with an acid capacity of 5.62 mmol/g.

Figure 2 shows the increase in Lu(III) sorption with increasing contact time calculated as percent and loading per gram on the phosphinic acid. Equilibrium is reached at 60 min with complete Lu(III) recovery from  $\leq 0.50$  mM Lu(III) solutions. At 1.0 mM Lu(III), complete recovery is achieved at 120 min with its curve being less sharp than those at lower concentrations. At 30 min, 98.5%, 91.5%, 87.3% and 56.6% Lu(III) is recovered from 0.033 mM (0.10 mN), 0.10 mM, 0.50 mM and 1.0 mM Lu(III), respectively. At 0.10 mM Lu(III), the concentration decreases to 0.1 mg/L within 1 h; at 0.50 and 1.0 mM, 2 and 4 h contact times are needed to reach that level. A longer contact time is needed for complete recovery at the higher Lu(III) concentration.

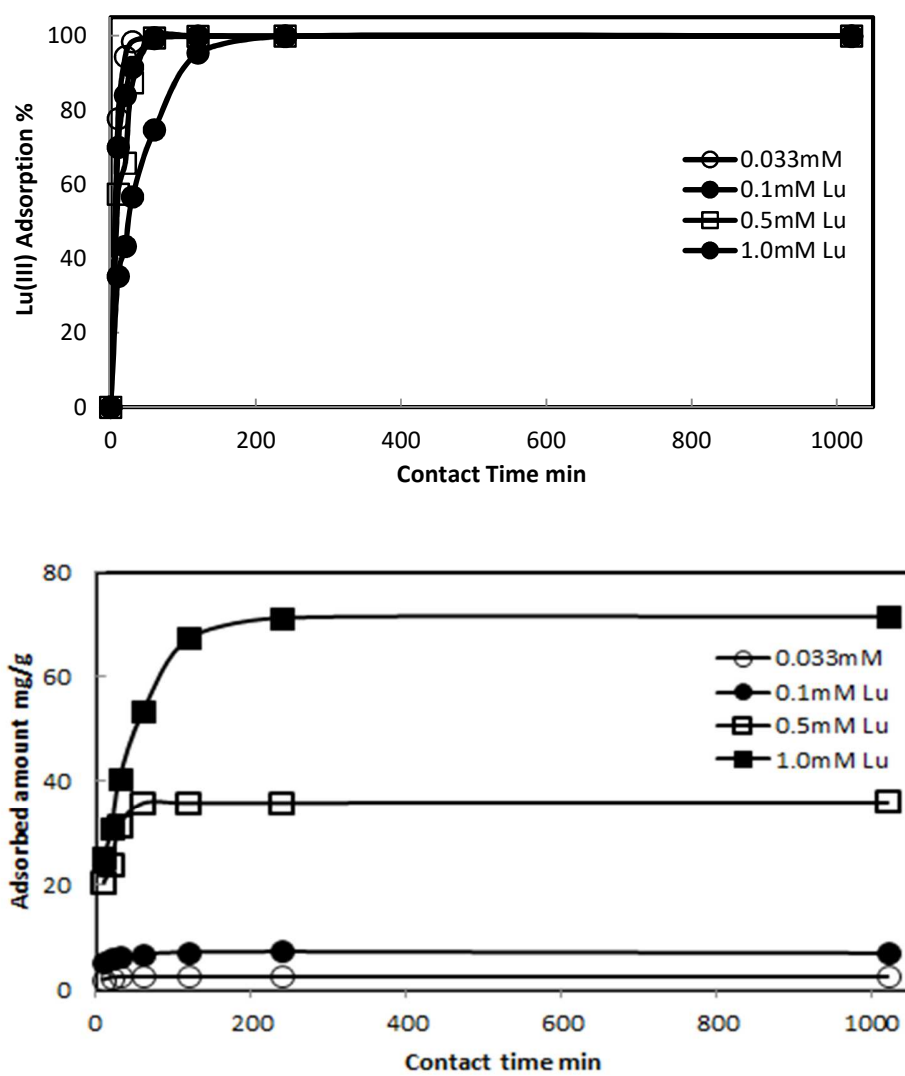


Fig. 2. Lu(III) sorption on phosphinic acid beads from 0.01M HNO<sub>3</sub> as a function of time measured in percent (top) and amount (bottom).

Adsorption on the sulfonic acid is much more rapid. Within 30 min, > 93% Lu(III) is removed regardless of the initial concentration (Fig. 3). The Lu(III) is completely adsorbed in < 1 h.

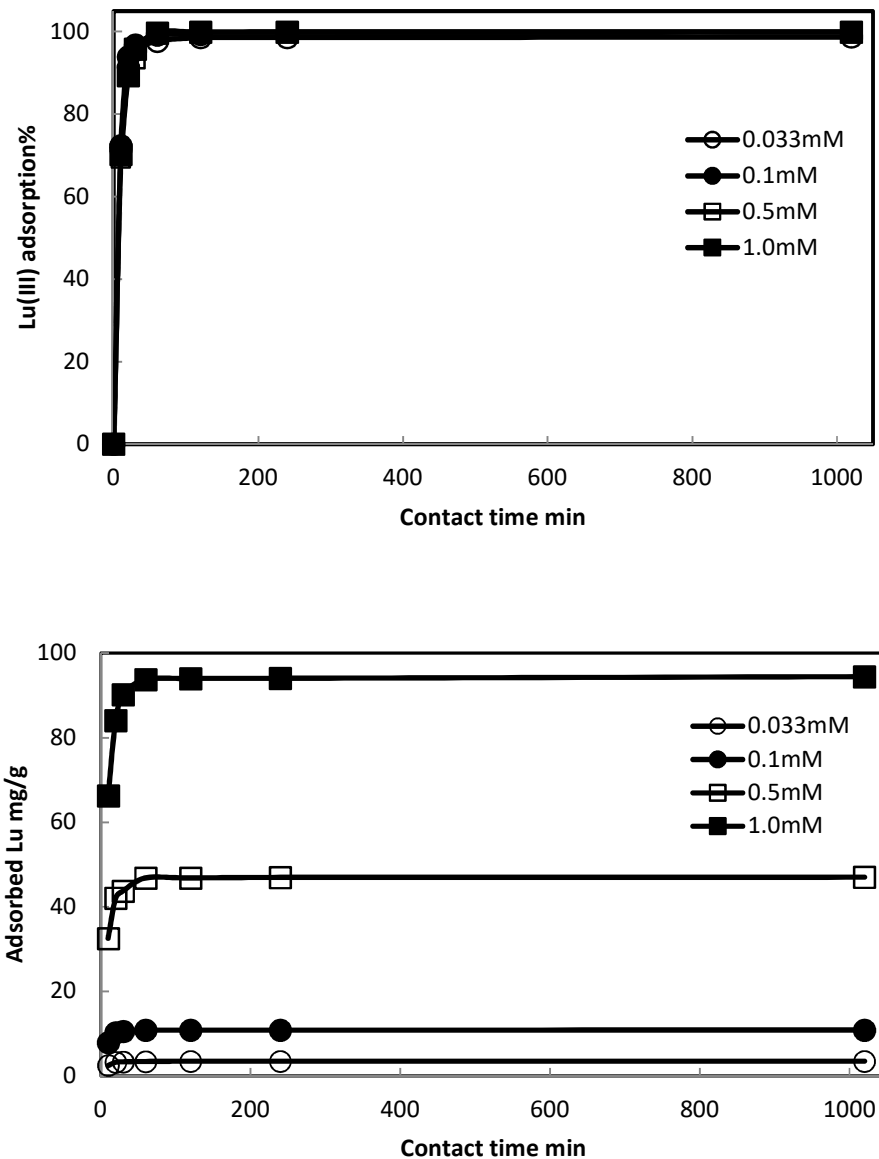


Fig. 3. Lu(III) sorption on sulfonic acid beads from 0.01M HNO<sub>3</sub> as a function of time measured in percent (top) and amount (bottom).

Figure 4 shows the result of sequentially contacting the phosphinic and sulfonic acid beads with Lu(III) five times with 50 mL of 0.50 mM Lu(III). The sulfonic acid quantitatively adsorbs the Lu(III) each time but adsorption by the phosphinic acid decreases from 98.6% to 28.9%; as will be discussed, this becomes important to understanding the sorption mechanism.

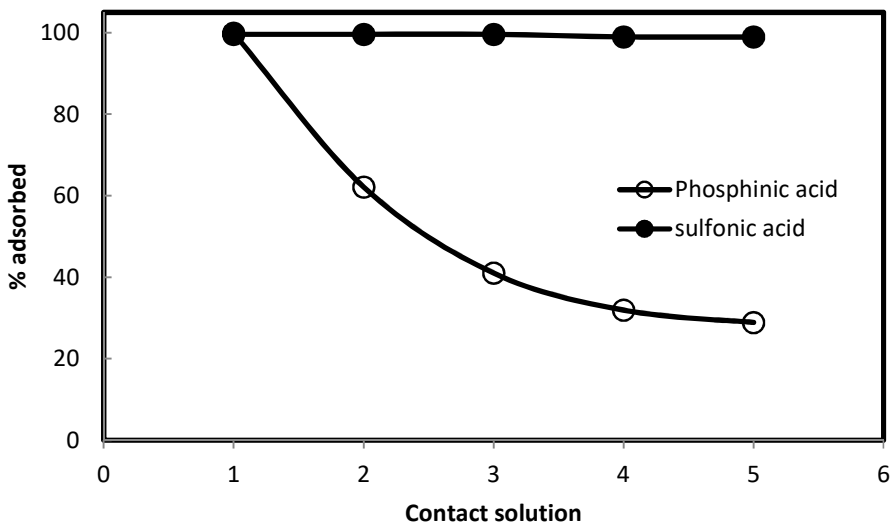


Fig. 4. Sequential contact (five times) of 0.50 mM Lu(III) with phosphinic and sulfonic acid beads

Lu(III) sorption by the phosphinic acid increases significantly when it is shaken with  $\text{H}_2\text{O}$  for 17 h after contacting the Lu(III) solution (Fig. 5). The percent adsorbed is 99.9% in the first two contacts, then decreases to 92.2%, 80.4% and 43.3% by the fifth contact. The water washes do not remove Lu(III) from the beads since it is not detected in solution.

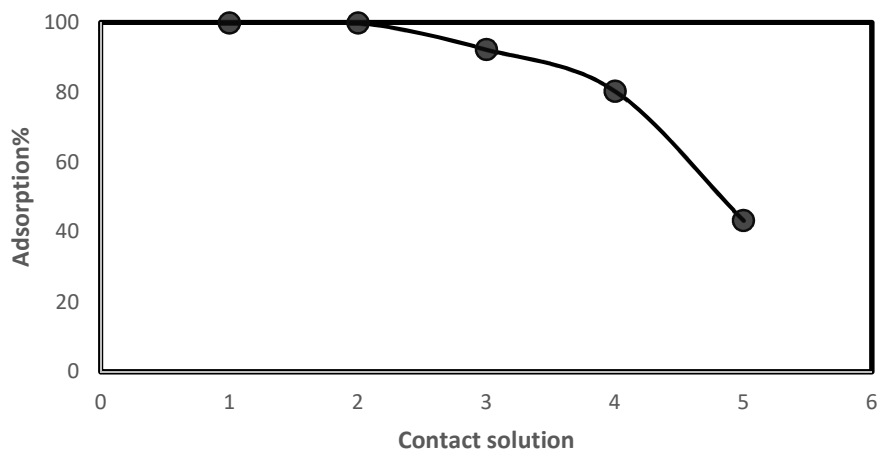


Fig. 5. Sequential contact (five times) of 0.50 mM Lu(III) with phosphinic acid beads and a water wash between each interval

**Effect of Lu(III) sorption on phosphinic acid.** Figure 6 shows changes in the ATR spectrum of the phosphinic acid before and after contact with 0.033 mM Lu(III). The bands at 951 and 968  $\text{cm}^{-1}$  are assigned to P-O(H) while those at 1125 and 1168  $\text{cm}^{-1}$  are assigned to P=O.<sup>36</sup> When the phosphinic acid is contacted with 0.033 mM Lu(III) for 1 h, the spectrum is comparable to that of the free ligand but with decreased intensities, most notably of the P-O(H) bands, and the P=O band at 1168 shifts to 1160  $\text{cm}^{-1}$ . At a 17 h contact, the spectrum becomes more similar to the metal-free ligand as the intensity of the P-O(H) band increases compared to that after 1 h, though it is still of lower intensity than the Lu-free ligand.

The effect of contact on the phosphinic acid by 1.0 mM Lu(III) is shown in Figure 7. At a contact of only 10 min, the intensities of the P-O(H) bands decrease significantly, especially at 951  $\text{cm}^{-1}$  which weakens to a shoulder. The P=O band, initially at 1168 and 1125  $\text{cm}^{-1}$ , shifts to 1133  $\text{cm}^{-1}$  with little change in intensity. Additionally, sufficient loading now occurs so that a new band at 1056 with medium intensity appears which is assigned to POO(Lu). The spectrum is similar when the contact time increases to 4 h (and to 17 h (not shown)).

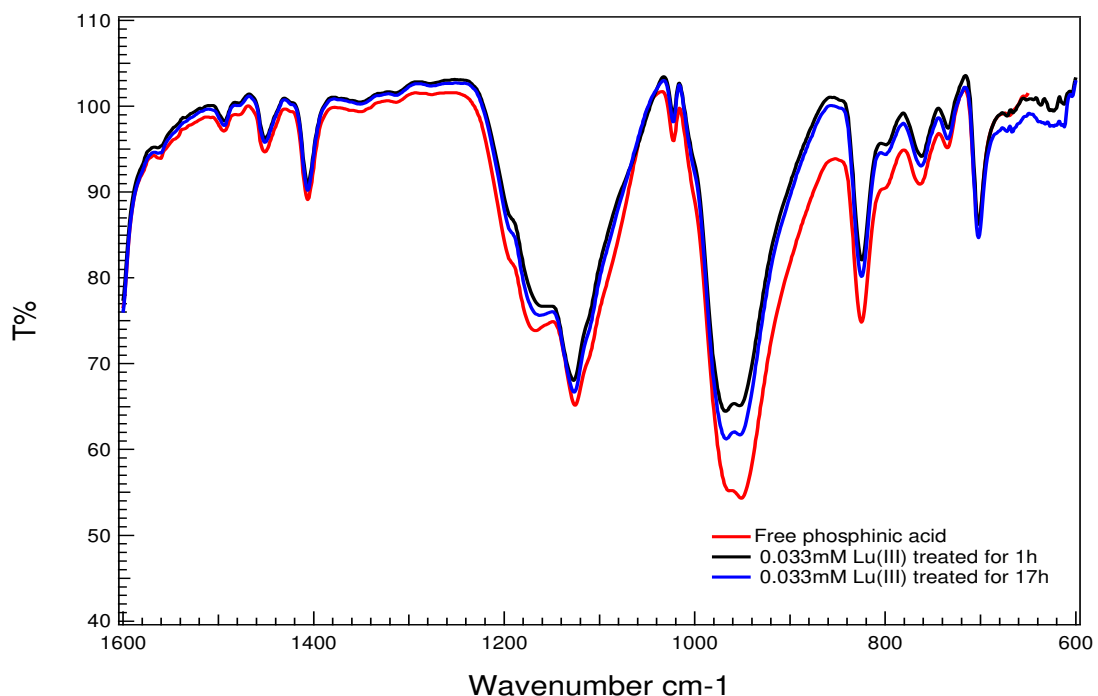


Fig. 6. ATR-FTIR spectrum of phosphinic acid before and after contact with 0.033 mM Lu(III)

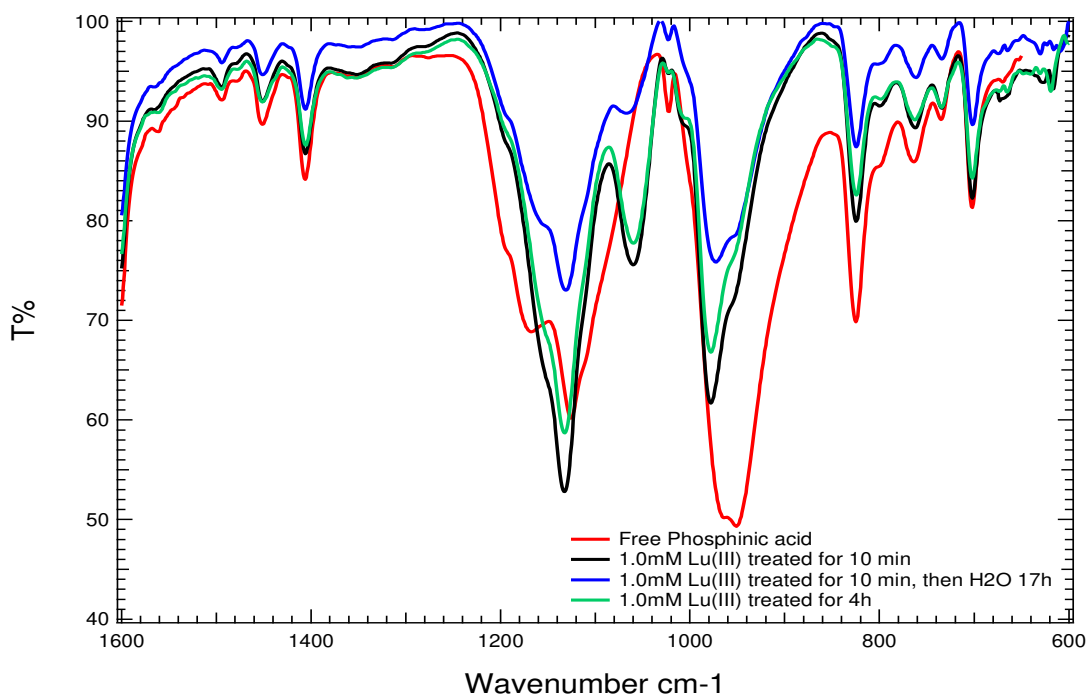


Fig. 7. ATR-FTIR spectrum of phosphinic acid before and after contact with 1.0 mM Lu(III)

Figure 7 also shows the effect of water treatment on the ATR spectrum of phosphinic acid after contact with 1.0 mM Lu(III). Removing the Lu(III) solution and shaking the beads with water for 17 h results in a different spectrum: The P=O band remains essentially unchanged but the intensity of the POO(Lu) band decreases while the intensities of the P-O(H) band at 973 and 951  $\text{cm}^{-1}$  increase. Water treatment thus gives a spectrum that approaches the appearance of Lu-free phosphinic acid even though no Lu(III) is detected in the water after the 17 h shake indicating that it did not wash off the beads.

**Effect of Lu(III) adsorption on the sulfonic acid.** Changes accompanying contact of the sulfonic acid with 1.0 mM Lu(III) for 17 h are shown in Figure 8. The ATR spectrum shows four strong bands at 1166, 1124, 1032 and 1006  $\text{cm}^{-1}$ . The bands at 1166 and 1032  $\text{cm}^{-1}$  are assigned to the asymmetric and symmetric sulfonate bands.<sup>37,38</sup> The sulfonic acid is strongly acidic and dissociates to hydronium ions.<sup>39</sup> Upon contacting Lu(III), ion exchange readily occurs with little change in the ATR since the hydrated Lu(III) does not disrupt the  $\text{SO}_3^-$  structure originally bound to the hydronium ion.<sup>40</sup> Exchange occurs, though, since elemental analysis of the Lu(III)-loaded polymer gives 123.4 mg Lu(III) per gram polymer.

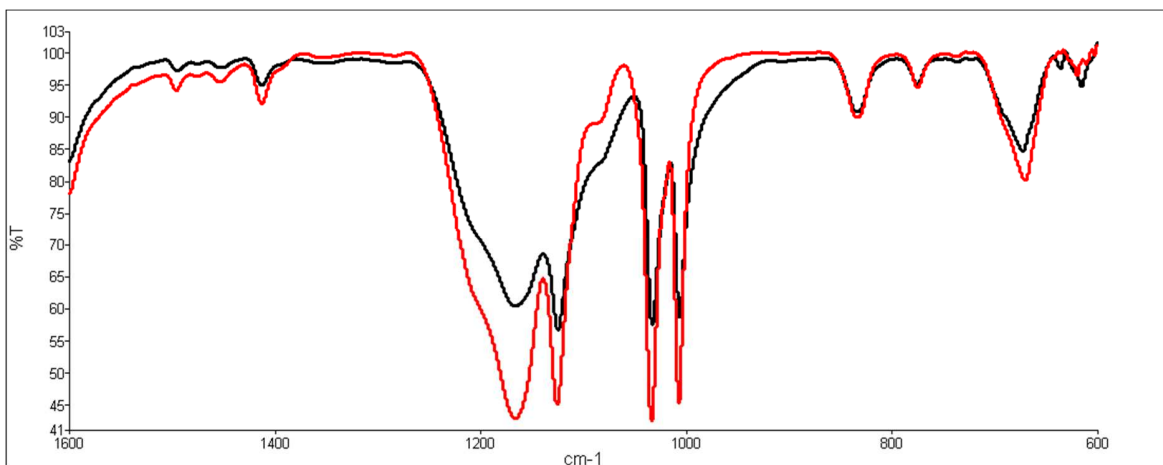


Fig. 8. ATR-FTIR spectrum of sulfonic acid before and after contact with 1.0 mM Lu(III)  
(Black: Lu(III)-free sulfonic acid; Red: 17 h contact with Lu(III))

**Effect of crosslinking.** Metal ion affinities are known to depend on the concentration of organophosphorus acids in solvent extraction<sup>41</sup> and ion exchange.<sup>42</sup> Ligand density can thus be expected to affect the extent of Lu(III) adsorption within beads. This was tested with Amberlite XAD-4 onto which phosphinic acid ligands were immobilized. XAD-4 is a highly crosslinked commercially available macroporous polymer bead that consists of 80–85 wt% DVB and 15–20 wt% ethylvinylbenzene.<sup>43</sup> Its tight network was evident in a swelling study that showed its volume to increase by 35% in toluene while the gel beads crosslinked with 2% DVB swelled by 250%. It was phosphinated with the same procedure used for the gel but had a phosphorus capacity of only 2.69 mmol/g due to limited accessibility of the phenyl rings.

Figure 9 compares the Lu(III) sorption kinetics from 0.033 mM Lu(III) in 0.01 M HNO<sub>3</sub> for the gel- and XAD-4-supported phosphinic acids. The sorption rates for both were rapid during the first hour and equilibrium was reached in 2 h with 98.5% Lu(III) adsorbed on the gel and 92.9% on the XAD-4. Though much more highly crosslinked, the XAD-4 has rapid kinetics due to its macroporosity.

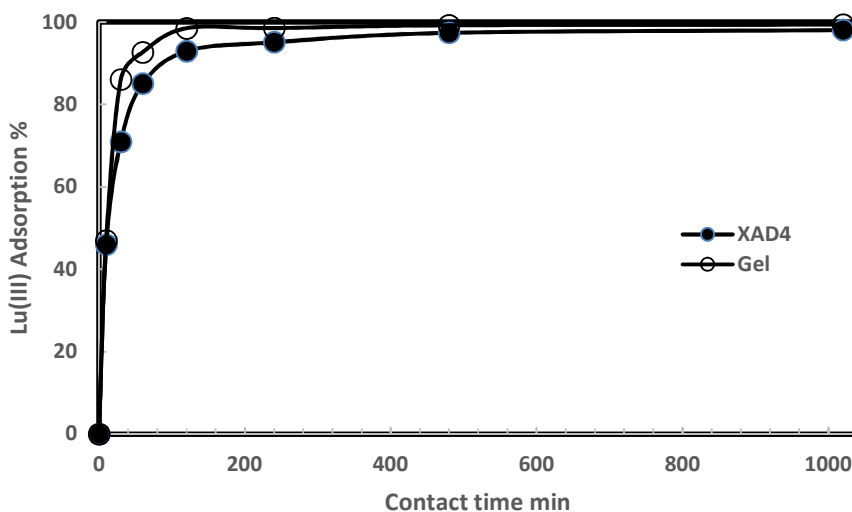


Fig. 9. Lu(III) sorption on gel and XAD-4 phosphinic beads from 0.01 M HNO<sub>3</sub> as a function of time

Though the gel and XAD-4 phosphinic acids behave similarly with respect to Lu(III) affinity and kinetics, the changes in the ATR spectra suggest different complexation mechanisms. Fig. 1S (Supplementary Information) shows the variation in ATR spectra of XAD-4 phosphinic acid at different Lu(III) contact times. The ATR spectrum of the metal-free polymer (Fig. 1A) has P=O and P-O(H) bands as discussed above. The concentration of the Lu(III) contact solution was increased to 10 mM for sufficient Lu(III) to be loaded and seen on the spectrum due to the lower phosphorus capacity. Upon contact for 10 min, the P=O and P-O(H) bands change to positions almost identical with those of the gel polymer: The P=O band shifts to 1136 cm<sup>-1</sup> while the P-O(H) band at 982 cm<sup>-1</sup> becomes much weaker (Fig. 1B). A new band assigned to POO(Lu) forms at 1065 cm<sup>-1</sup>. Further treatment of the Lu-loaded polymer with water for 17 h changes its spectrum (Fig. 1b) as the band intensities of P-O(H) at 934, 981 cm<sup>-1</sup> become stronger than in Fig. 1B and comparable to the POO(Lu) band at 1062 cm<sup>-1</sup>. The P=O band shifts upward to 1144 cm<sup>-1</sup> from 1136 cm<sup>-1</sup>. An increase of Lu(III) contact time to  $\geq 0.50$  h and subsequent water washes cause little change in the spectra (Fig. 1S: C, c, D, d, E, e). These results are compared to the gel polymer in the next section. Table 1 summarizes the changes in band positions upon Lu(III) loading and water treatment.

Table 1. Phosphinate bands before and after contact with 10 mM Lu(III) and water wash

	P=O	P-O(H)	POO(Lu)	P=O	P-O(H)	POO(Lu)	
Time	<b>after Lu(III) contact</b>			<b>after water contact</b>			
<b>XAD-4 phosphinic acid</b>							
0	1167, 1125	973, 948					
10 min	1136	982, 931	1065	1144	981, 934	1062	
0.50 h	1135	983, 932	1062	1134	983, 938	1058	
1 h	1135	982, 939	1061	1134	982, 939	1060	
17 h	1135	982, 939	1061	1134	983, 933	1060	
<b>Gel phosphinic acid</b>							
0	1167, 1126	964, 951					
10 min	1133	980, 952	1060	1166, 1128	966, 952		
0.50 h	1133	979, 952	1060	1151, 1129	974, 952	1069	
1 h	1133	979	1060	1154, 1131	972, 952	1069	
4 h	1133	979	1058	1154, 1131	973, 952	1067	
17 h	1133	980	1057	1133	980	1057	

#### 4. Discussion

The phosphinic and sulfonic acid ligands adsorb Lu(III) but at significantly different rates (Figs. 2 – 4). Adsorption on the sulfonic acid is complete within 30 min and a concentration change from 0.033 to 1.0 mM Lu(III) has little effect on the kinetics. Though polystyrene-based gel beads have little surface area, all of the sulfonate ligands remain accessible to the ions and adsorption is rapid even when the beads are contacted five times consecutively with 50 mL of 0.50 mM Lu(III). The phosphinic acid, with the same polymer backbone and a similar acid capacity, has slower kinetics than the sulfonic acid and depends on the Lu(III) concentration. Figs. 4 and 5 indicate that not all of the ligands are available when the beads are contacted consecutively with 0.50 mM Lu(III). A water wash after each of the contacts with Lu(III) solution increases the total amount adsorbed from 51.7% to 83.1% by increasing the availability of adsorption sites (*vide infra*).

Time-dependent adsorption onto solids can be described in terms of pseudo-first and second order models<sup>44,45</sup> but they cannot explain the differences seen here between the phosphinic and sulfonic acids. A detailed insight was, however, provided by ATR-FTIR spectroscopy that

reports changes only on the surface of the polymer. With the sulfonic acid, there is little variation in the ATR spectra upon Lu(III) adsorption (Fig. 9). Though Lu(III) exchanges with the  $\text{H}_3\text{O}^+$  at the acid site, the similarity in the spectra before and after exchange suggests no new ionic bond is formed. Treatment of the sulfonic acid with 0.10 M NaOH supports this conclusion since, again, there is little difference in the ATR-FTIR spectra as well as the volume of the beads in acid and base conditions given that the sulfonic acid ligand is ionized because of its strong acidity (the analogous p-toluenesulfonic acid has a pKa of -2.7).<sup>46</sup> The hydrated  $-\text{SO}_3^- \text{H}_3\text{O}^+$  makes the bonds in the sulfonate group equivalent and there is no  $\text{S}=\text{O} / \text{S}-\text{O}$  present.<sup>39</sup> The hydronium ion is thus not strongly bound to the oxygen and is mobile within the wet beads to form a solvent-separated ion pair with the delocalized negative charge of the sulfonate ion. The percent solid (23.9%) confirms that the ligand is hydrophilic resulting in a low resistance to ion exchange between the solid and aqueous phases.

Strong hydrogen bonding in soluble acidic phosphorus-based ligands has been shown through their self-association<sup>47</sup> and the metal ion binding of complexants such as bis(2,4,4-trimethylpentyl)phosphinic acid as dimers rather than monomers.<sup>48</sup> Most importantly, the  $\text{P}=\text{O}$  bands in the phosphinic acid ligand at 1167 and 1126  $\text{cm}^{-1}$  that can be interpreted as symmetric and asymmetric stretching bands can equally well be interpreted, with significant literature precedent, as arising from differences in hydrogen bonding to the phosphoryl oxygen.<sup>27</sup> Comparing the bathochromic shift of the phosphoryl band in immobilized  $-\text{CH}_2\text{P}(\text{O})(\text{OH})_2$  with that of the phosphinic acid  $-\text{PH}(\text{O})\text{OH}$  also supports hydrogen bonding in phosphorus acid ligands.<sup>30</sup> The phosphinic acid is of intermediate acidity with a pKa of 3.2<sup>49</sup> indicating that the proton remains associated with the phosphinate portion of the ligand as  $\text{P}(\text{O})\text{OH}$  (Fig. 6). Contacting the beads with 0.10 M NaOH swells their volume by a factor of 2.3, unlike with the sulfonic acid; the sulfonate ligand is thus already present with a loose association to the hydronium ion while the highly hydrophilic phosphinate anion forms only after exchange with  $\text{Na}^+$ . When the phosphinic acid contacts Lu(III), exchange occurs to form the ionically bound  $\text{POO}(\text{Lu})$ , which is evident in the new band at 1056  $\text{cm}^{-1}$  and a related decrease in the  $\text{P}-\text{O}(\text{H})$  band intensity (Fig. 7). Unlike its swelling with NaOH, contacting the phosphinic acid with 0.02 M Lu(III) decreases the volume of the beads slightly; its corresponding adsorption of 0.72 mmol

Lu(III) per gram polymer suggests a stronger interaction with the Lu(III) than hydrogen bonding in the metal-free ligand. A volume decrease with chelating resins upon metal adsorption has been observed<sup>50</sup> and metal “crosslinking” of bifunctional phosphates leads to polymerization<sup>51</sup> and aggregation.<sup>52</sup>

Though the sulfonic and phosphinic acids can exchange for Lu(III), the availability of acid sites is not the same. The sulfonate’s ion pair structure as well as its hydrophilicity makes the sites equally accessible (Fig. 10). The solvent-separated  $\text{H}_3\text{O}^+$  exchanges rapidly at all sites and a change in Lu(III) concentration has little effect on the sorption kinetics (Figs. 3 and 4).

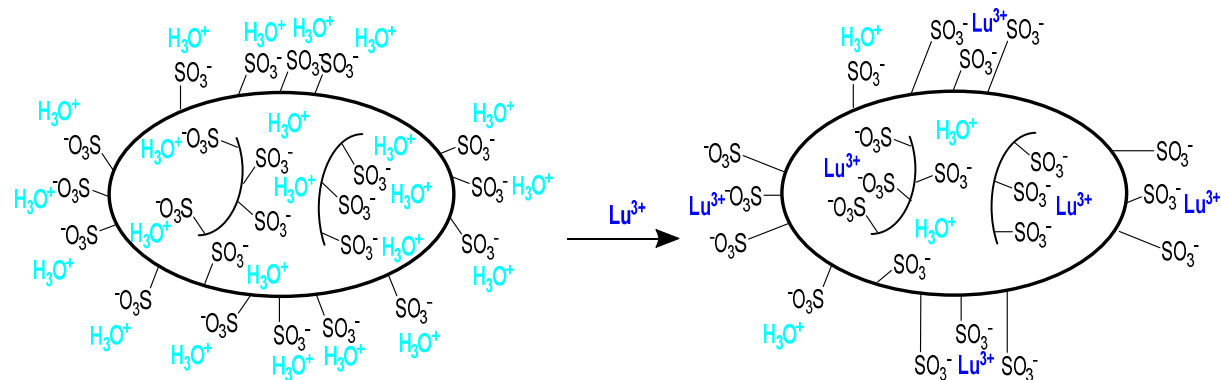


Fig. 10. Lu(III) sorption on the sulfonic acid

The phosphinic acid behaves differently from the sulfonic acid. The change in the ATR spectrum within 10 min of Lu(III) contact indicates unhindered access to the surface ligands (Fig. 7). Though adsorption increases with contact time (Fig. 2), there is no further change in the ATR spectrum up to 17h. With the limited number of sites on the bead surface, increasing the Lu(III) concentration slows adsorption since hydrogen bonding limits accessibility to the interior sites. Lu(III) can be completely removed from solution (Fig. 2) but a longer contact time is needed at 1.0 mM than 0.033 mM. Thus the ATR spectra support the hypothesis that phosphinic acid ligands in gel beads are such that the outer ligands are more accessible than those in the interior.

Lu(III) adsorption into the interior involves breaking hydrogen bonds between the P-OH and P=O moieties and the question becomes whether the Lu(III) in the interior comes directly from solution or from those initially adsorbed on the surface. This is clarified by ATR spectra after

beads contacted with 1.0 mM Lu(III) for 10 min are treated with water (Fig. 7). The increased intensity of the P-OH band and decreased intensity of the POO(Lu) band indicate that more ligands on the surface become available for adsorption since there is no release of Lu(III) into the water. The changes are due to the ion's mobility in which the Lu(III) initially adsorbed on the surface moves into the interior to take up the inner sites and makes the surface sites again available. The decrease of the P-OH intensity at 17 h in Fig. 6 also suggests movement of initially adsorbed Lu(III) from the surface. This type of "hopping" mechanism is often invoked in membrane research.<sup>53</sup> ATR spectra thus allow us to determine that Lu(III) adsorption on the phosphinic acid occurs in two steps: Lu(III) in aqueous solution initially binds to the outermost ligands, then the Lu(III) moves from those sites to the interior leaving the outer sites available for additional adsorption. This is summarized by Fig. 11.

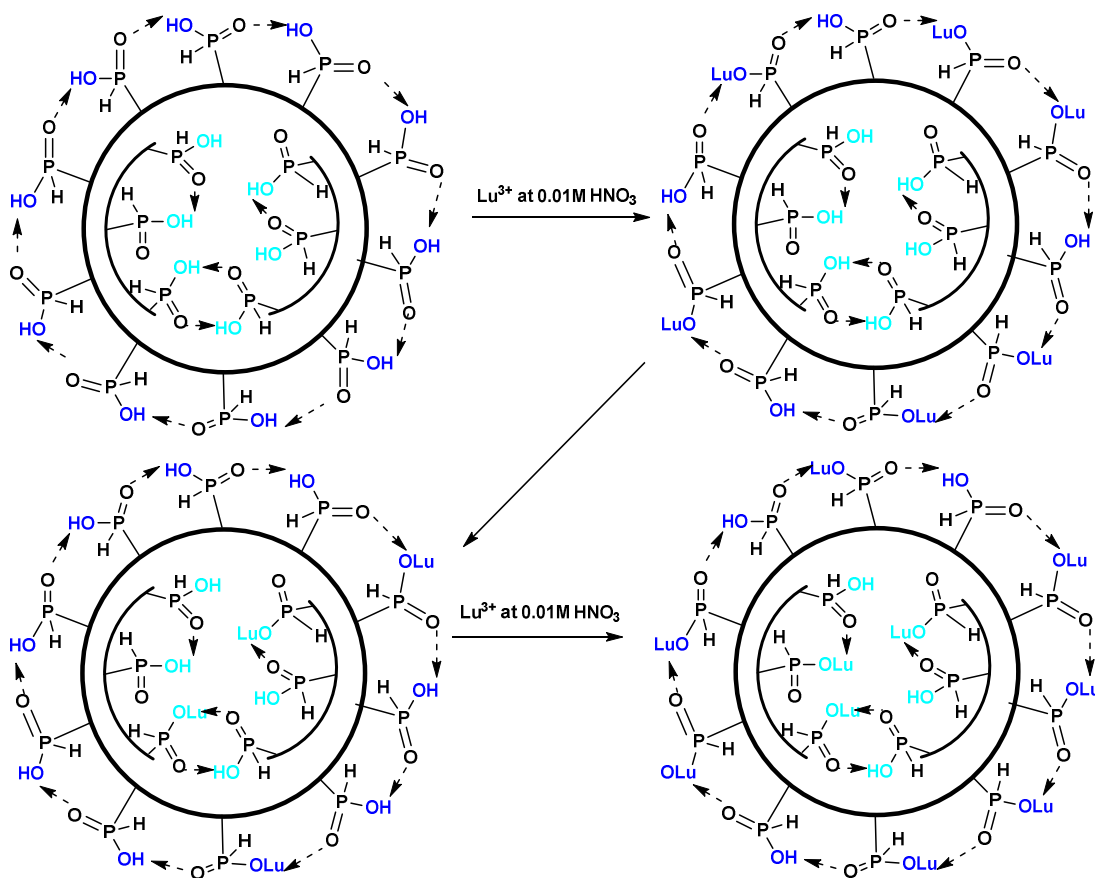


Fig. 11. Lu(III) sorption on the phosphinic acid

Changes in the ATR spectra of XAD-4 upon Lu(III) adsorption support both proton exchange and P=O coordination in metal binding. The intensity of its bands (939, 982 cm<sup>-1</sup>) corresponding to the P-O(H) weakens, suggesting that nearly all the acid P-O(H) groups on the surface react with Lu(III). Meanwhile the P=O shifts down to 1135 from 1167 cm<sup>-1</sup> indicating coordination of the P=O bond with the adsorbed metal ions. The POO(Lu) is evident at 1065 cm<sup>-1</sup>. Its macroporous structure makes more surface ligands accessible to metal ions. Lu(III) adsorption in 10 min consumes nearly all available sites. Further water treatment of Lu(III)-loaded XAD-4 changes somewhat its P-O(H) band intensity but the change is less pronounced than with the gel, indicative of a decreased mobility and decreased hopping.

With the gel, the similarity in ATR spectra obtained at 10 min and 17 h contact confirm a rapid reaction between Lu(III) and surface phosphinate ligands. The ATR reflects only surface adsorption at the short 10 min contact. Water treatment restores the phosphinic acid bands, indicating re-availability for Lu(III) adsorption on the surface. The corresponding disappearance of the POO(Lu) band is not due to elution of adsorbed Lu(III) but, rather, its diffusion into the interior. Strong intermolecular forces hinder the interior vacant binding sites from being occupied in a short time but the nearly identical ATR spectra of the Lu(III)-loaded gel after water treatment with that of the free ligand indicate that the adsorbed Lu(III) diffuses into the bulk phase and the newly vacant sites on the surface can be utilized again by the Lu(III) in solution.

## 5. Conclusions

Changes in the ATR spectra upon binding Lu(III) to the gel phosphinic acid before and after water treatment shows that adsorption occurs by diffusion from the surface to the interior. Binding to the polymer interior is more difficult than with surface ligands due to intermolecular hydrogen bonding. Surface ligands are reactive, accessible and form complexes rapidly with Lu(III) in aqueous solutions. Inner ligands, though reactive, gain access more slowly to Lu(III) ions because they come from those initially bound to surface ligands. The inner ligands do not react directly with the Lu(III) in aqueous solution. Lu(III)-reacted surface ligands release their

Lu(III) to inner ligands and react again with Lu(III) in solution. Initially adsorbed Lu(III) on the phosphinate is mobile and metal ion adsorption is accompanied by hydrogen bond-breaking and Lu(III) bond-making. The readily ionizable sulfonic acid rapidly exchanges with Lu(III) due to its low pKa. The hopping mechanism of transport becomes evident with the lower phosphorus capacity of the XAD-4.

### **Acknowledgement**

We acknowledge support from the Chemical Sciences, Geosciences and Biosciences Division, Office of Basic Energy Sciences, Office of Science, U.S. Department of Energy through grant DEFG02-02ER15287.

### **Reference**

---

<sup>1</sup> Besser, J.M.; Brumbaugh, W.G.; Ingersoll, C.G. Characterizing toxicity of metal-contaminated sediments from mining areas, *Appl. Geochem.* 2015, 57, 73-84.

<sup>2</sup> Zhang, L.; Xu, Z. A review of current progress of recycling technologies for metals from waste electrical and electronic equipment, *J. Cleaner Production*, 2016, 127, 19-36.

<sup>3</sup> Moussa, M.; Ndiaye, M.M.; Pinta, T.; Pichon, V.; Vercouter, T.; Delaunay, N. Selective solid phase extraction of lanthanides from tap and river waters with ion imprinted polymers, *Anal. Chim. Acta* 2017, 963, 44-52.

<sup>4</sup> Kantipuly, C.; Katragadda, S.; Chow, A.; Gesser, H.D. Chelating polymers and related supports for separation and preconcentration of trace metals, *Talanta* 1990, 37, 491-517.

<sup>5</sup> Chauhan, G.; Pant, K.K.; Nigam, K.D.P. Chelation technology: a promising green approach for resource management and waste minimization, *Environ. Sci. - Processes & Impacts*, 2015, 17, 12-40.

---

<sup>6</sup> Alexandratos, S. D. From ion exchange resins to polymer-supported reagents: an evolution of critical variables, *J. Chem. Tech. Biotech.* 2018, 93, 20-27.

<sup>7</sup> Ke, F.; Jiang, J.; Li, Y.Z.; Liang, J.; Wan, X.C.; Ko, S. Highly selective removal of Hg<sup>2+</sup> and Pb<sup>2+</sup> by thiol-functionalized Fe<sub>3</sub>O<sub>4</sub>@metal-organic framework core-shell magnetic microspheres, *Appl. Surf. Sci.* 2017, 413, 266-274.

<sup>8</sup> Plazinski, W.; Rudzinski, W. Kinetics of Adsorption at Solid/Solution Interfaces Controlled by Intraparticle Diffusion: A Theoretical Analysis, *J. Phys. Chem. C*, 2009, 113, 12495–12501.

<sup>9</sup> Juang, R.S.; Lin, H.C. Metal sorption with extractant - impregnated macroporous resins. 1. Particle diffusion kinetics, *J. Chem. Tech. Biotech.* 1995, 62, 132 – 140.

<sup>10</sup> Chiarle, S.; Ratto, M.; Rovatti, M. Mercury removal from water by ion exchange resins adsorption, *Water Res.* 2000, 34, 2971-2978.

<sup>11</sup> Ho, Y.S.; McKay, G. The kinetics of sorption of divalent metal ions onto sphagnum moss peat, *Water Res.* 2000, 34, 735-742.

<sup>12</sup> Ho, Y.S. Review of second-order models for adsorption systems, *J Hazard. Mater.* 2006, B136, 681–689.

<sup>13</sup> Wirth, H.; Unger, K.K.; Hearn, M.T.W. Influence of ligand density on the properties of metal-chelate affinity supports, *Anal. Biochem.* 1993, 208, 16-25.

<sup>14</sup> Gerbier, S.A.; Desert, S.; Kryswicki, T.G.; Larpent, C. Ultrafine selective metal-complexing nanoparticles: Synthesis by microemulsion copolymerization, binding capacity, and ligand accessibility, *Macromolecules* 2002, 35, 1644-1650.

<sup>15</sup> Beatty, S.T.; Fischer, R.J.; Hagers, D.L.; Rosenberg, E. A comparative study of the removal of heavy metal ions from water using a silica-polyamine composite and a polystyrene chelator resin, *Ind. Eng. Chem. Res.* 1999, 38, 4402 -4408.

<sup>16</sup> Sengupta, A.K.; Zhu, Y. Metals sorption by chelating polymers: A unique role of ionic strength, *AIChE J.* 1992, 38, 153-157.

---

<sup>17</sup> Reddad, Z.; Gerente, C.; Andres, Y.; Le Cloirec, P. Adsorption of several metal ions onto a low-cost biosorbent: Kinetic and equilibrium studies, *Environ. Sci. Technol.*, 2002, 36, 2067–2073.

<sup>18</sup> Zhu, X.; Alexandratos, S.D. Development of a new ion-exchange/coordinating phosphate ligand for the sorption of U(VI) and trivalent ions from phosphoric acid solutions, *Chem. Eng. Sci.* 2015, 127, 126-132; Helfferich, F. Ion-exchange kinetics. V. Ion exchange accompanied by reactions, *J. Phys. Chem.* 1965, 69, 1178-1187.

<sup>19</sup> Klein-Hitpass, M.; Lynes, A.D.; Hawes, C.S.; Byrne, K.; Schmitt, W.; Gunnlaugsson, T. A Schiff-base cross-linked supramolecular polymer containing diiminophenol compartments and its interaction with copper(II) ions, *Supramolec. Chem.* 2018, 30, 93-102.

<sup>20</sup> Rahman, M.L.; Mandal, B.H.; Sarkar, S.M.; Wahab, N.A.A.; Yusoff, M.M.; Arshad, S.E.; Musta, B. Synthesis of poly(hydroxamic acid) ligand from polymer grafted khaya cellulose for transition metals extraction, *Fibers and Polymers* 2016, 17, 521-532.

<sup>21</sup> Vyprachticky, D.; Mikes, F.; Lokaj, J.; Pokorna, V.; Cimrova, V. Resonance energy transfer from quinolinone modified polystyrene-block-poly(styrene-alt-maleic anhydride) copolymer to terbium(III) metal ions, *J. Luminesc.* 2015, 160, 27-34.

<sup>22</sup> von Leupoldt, A.W.; Forster, C.; Fiedler, T.J.; Bings, N.H.; Heinze, K. Proton and electron transfer to a polymer-supported nitrido molybdenum(vi) complex, *Eur. J. Inorg. Chem.* 2013, 36, 6079-6090.

<sup>23</sup> Mini, V.; Archana, K.; Raghu, S.; Sharanappa, C.; Devendrappa, H. Nanostructured multifunctional core/shell ternary composite of polyaniline-chitosan-cobalt oxide: Preparation, electrical and optical properties, *Mater. Chem. Phys.* 2016, 170, 90-98.

<sup>24</sup> Vieira, R.S.; Meneghetti, E.; Baroni, P.; Guibal, E.; Gonzalez de la Cruz, V.M.; Caballero, A.; Rodriguez-Castellon, E.; Beppu, M.M. Chromium removal on chitosan-based sorbents - An EXAFS/XANES investigation of mechanism, *Mater. Chem. Phys.* 2014, 146, 412-417.

<sup>25</sup> Hind, A.R.; Bhargava, S.K.; McKinnon, A. At the solid/liquid interface: FTIR/ATR the tool of choice, *Adv. Colloid Interface Sci.* 2001, 93, 91-114.

---

<sup>26</sup> Sperline, R.P.; Muralidharan, S.; Freiser, H. In situ determination of species adsorbed at a solid-liquid interface by quantitative infrared attenuated total reflectance spectrophotometry, *Langmuir*, 1987, 3, 198–202.

<sup>27</sup> Alexandratos, S.D.; Zhu, X. Through-bond communication between polymer-bound phosphinic acid ligands and trivalent metal ions probed with FTIR spectroscopy, *Vibr. Spec.* 2018, 95, 80-89.

<sup>28</sup> Pospiech, B.; Chagnes, A. Highly selective solvent extraction of Zn(II) and Cu(II) from acidic aqueous chloride solutions with mixture of Cyanex 272 and Aliquat 336, *Sep. Sci. Tech.* 2015, 50, 1302-1309.

<sup>29</sup> Yang, Y.; Alexandratos, S.D. Affinity of polymer-supported reagents for lanthanides as a function of donor atom polarizability, *Ind. Eng. Chem. Res.* 2009, 48, 6173-6187.

<sup>30</sup> Alexandratos, S.D.; Zhu, X. The role of polarizability in determining metal ion affinities in polymer-supported reagents: monoprotic phosphates and the effect of hydrogen bonding, *New J. Chem.*, 2015, 39, 5366-5373.

<sup>31</sup> Herlinger, A.W.; Ferraro, J.R.; Garcia, J.A.; Chiarizia, R. A far-infrared study and investigation of the difference between the asymmetric and symmetric POO- stretching frequencies in metal diphosphonate complexes, *Polyhedron* 1998, 17, 1471-1475.

<sup>32</sup> Freire, R.O.; da Costa Jr., N.B.; Rocha, G.B.; Simas, A.M. Sparkle/AM1 Structure Modeling of Lanthanum (III) and Lutetium (III) Complexes, *J. Phys. Chem. A* 2006, 110, 5897-5900

<sup>33</sup> Ma, E.X.; Muralidharan, S.; Freiser, H.; Jiang, P.H. Kinetic behavior of lanthanide extraction with acidic phosphorus extractants, *J. Chem. Tech. Biotech.* 1996, 65, 81-85.

<sup>34</sup> Alexandratos, S.D.; Strand, M.A.; Quillen, D.R.; Walder, A.J. Synthesis and Characterization of Bifunctional Phosphinic Acid Resins, *Macromolecules*, 1985, 18, 829-835.

<sup>35</sup> Daniels, Y.; Zhu, X.; Alexandratos, S.D. Distinguishing between organic and inorganic phosphorus in hydroxyapatite by elemental analysis, *Microchem. J.* 2013, 110, 263-265.

---

<sup>36</sup> Kaizin, L.I.; Mason, G.W.; Peppard, D.F. Infrared spectral observation on the P=O group vibration of some homogeneous series of organic derivatives of P(V), *Spectrochim. Acta*, 1978, 34A, 57-61.

<sup>37</sup> Kujawski, W.; Nguyen, Q.T.; Neel, J. Infrared investigations of sulfonated ionomer membranes. I. Water–alcohol compositions and counterions effects, *J. Appl. Polym. Sci.*, 1992, 44, 951-958.

<sup>38</sup> Brijmohan, S.B.; Swier, S.; Weiss, R.A.; Shaw, M.T. Synthesis and characterization of cross-linked sulfonated polystyrene nanoparticles, *Ind. Eng. Chem. Res.* 2005, 44, 8039-8045.

<sup>39</sup> Pereira, M.R.; Yarwood, J. ATR-FTIR spectroscopic studies of the structure and permeability of sulfonated poly(ether sulfone) membranes. Part 1.-Interfacial water-polymer interactions, *J. Chem. Soc., Faraday Trans.*, 1996, 92, 2731-2735.

<sup>40</sup> Beyer, S.; Bai, J.H.; Blocki, A.M.; Kantak, C.; Xue, Q.R.; Raghunath, M.; Trau, D. Assembly of biomacromolecule loaded polyelectrolyte multilayer capsules by using water soluble sacrificial templates, *Soft Matter* 2012, 8, 2760-2768 (see Supplementary Material: “IR spectra of sulfonic acids often resemble those of sulfonic acid salts due to hydration to hydronium salts under normal working conditions”).

<sup>41</sup> Radhika, S.; Kumar, B.N.; Kantam, M.L.; Reddy, B.R. Liquid–liquid extraction and separation possibilities of heavy and light rare-earths from phosphoric acid solutions with acidic organophosphorus reagents, *Sep. Purif. Technol.* 2010, 75, 295-302.

<sup>42</sup> Lee, M.S.; Nicol, M.J. Removal of iron from cobalt sulfate solutions by ion exchange with Diphonix resin and enhancement of iron elution with titanium(III), *Hydrometallurgy* 2007, 86, 6–12.

<sup>43</sup> Kara D.; Fisher, A.; Hill, S.J. Comparison of some newly synthesized chemically modified Amberlite XAD-4 resins for the preconcentration and determination of trace elements by flow injection inductively coupled plasma-mass spectrometry (ICP-MS), *Analyst*, 2006, 131, 1232–1240.

<sup>44</sup> Rengaraj, S.; Moon, S.H. Kinetics of adsorption of Co(II) removal from water and wastewater by ion exchange resins, *Water Res.* 2002, 36, 1783–1793.

---

<sup>45</sup> Hu, X.; Li, Y.; Wang, Y.; Li, X.; Li, H.; Liu, X.; Zhang, P. Adsorption kinetics, thermodynamics and isotherm of thiocalix[4]arene-loaded resin to heavy metal ions, *Desalination* 2010, 259, 76–83

<sup>46</sup> Sun, Q; Farneth, W.E.; Hamer, M.A. Dimerization of  $\alpha$ -methylstyrene (AMS) catalyzed by sulfonic acid resins: A quantitative kinetic study, *J. Catal.* 1996, 164, 62-69.

<sup>47</sup> Cao, X.Y.; Zhang, J.; Weissmann, D.; Dolg, M.; Chen, X.B. Accurate quantum chemical modelling of the separation of  $\text{Eu}^{3+}$  from  $\text{Am}^{3+}/\text{Cm}^{3+}$  by liquid-liquid extraction with Cyanex272, *Phys. Chem. Chem. Phys.* 2015 17, 20605-20616; Marcus, Y.; Kertes, A.S. *Ion exchange and solvent extraction of metal complexes*, Wiley Interscience, London, 1969.

<sup>48</sup> Chiarizia, R.; McAlister, D.R.; Herlinger, A.W. Trivalent actinide and lanthanide separations by dialkyl-substituted diphosphonic acids, *Sep. Sci. Technol.* 2005, 40, 69-90.

<sup>49</sup> Egawa, H.; Nonaka, T.; Ikari, M. Preparation of macroreticular chelating resins containing dihydroxyphosphino and/or phosphono groups and their adsorption ability for uranium, *J. Appl. Polym. Sci.* 1984, 29, 2045–2055.

<sup>50</sup> Chen, C.; Chiang, C.L; Chen, C.R. Removal of heavy metal ions by a chelating resin containing glycine as chelating groups, *Sep. Purif. Technol.* 2007, 54, 396–403.

<sup>51</sup> Yellin, R.A.; Zangen, M.; Gottlieb, H.; Warshawsky, A. Bifunctional phosphoric acid-phosphine oxide extractants: Synthesis and complexes with uranium-(IV) and -(VI) and iron(III), *J. Chem. Soc. Dalton Trans.* 1990, 2081-2088.

<sup>52</sup> Chiarizia, R.; Barrans Jr., R.E.; Ferraro, J.R.; Herlinger, A.W.; McAlister, D.R. Aggregation of dialkyl-substituted diphosphonic acids and its effect on metal ion extraction, *Sep. Sci. Technol.* 2001, 36, 687-708.

<sup>53</sup> Jalili, J.; Borsacchi, S.; Tricoli, V. Proton conducting membranes in fully anhydrous conditions at elevated temperature: Effect of Nitrilotris(methylenephosphonic acid) incorporation into Nafion- and poly(styrenesulfonic acid), *J Membr. Sci.* 2014, 469, 162-173; Araki, K.; Maruyama, T.; Kamiya, N.; Goto, M. Metal ion-selective membrane prepared by surface molecular imprinting, *J. Chromatogr. B - Analytical Technologies in the Biomedical and Life Sciences* 2005, 818, 141-145.

Lu(III) sorption on the phosphinic acid polymer

